



HAL
open science

Piecewise log-normal approximation of size distributions for aerosol modelling

K. von Salzen

► **To cite this version:**

K. von Salzen. Piecewise log-normal approximation of size distributions for aerosol modelling. Atmospheric Chemistry and Physics Discussions, 2005, 5 (3), pp.3959-3998. hal-00301586

HAL Id: hal-00301586

<https://hal.science/hal-00301586>

Submitted on 18 Jun 2008

HAL is a multi-disciplinary open access archive for the deposit and dissemination of scientific research documents, whether they are published or not. The documents may come from teaching and research institutions in France or abroad, or from public or private research centers.

L'archive ouverte pluridisciplinaire **HAL**, est destinée au dépôt et à la diffusion de documents scientifiques de niveau recherche, publiés ou non, émanant des établissements d'enseignement et de recherche français ou étrangers, des laboratoires publics ou privés.

Piecewise log-normal approximation

K. von Salzen

Piecewise log-normal approximation of size distributions for aerosol modelling

K. von Salzen

Canadian Centre for Climate Modelling and Analysis, Meteorological Service of Canada, Victoria, British Columbia, Canada

Received: 7 April 2005 – Accepted: 5 May 2005 – Published: 14 June 2005

Correspondence to: K. von Salzen (knut.vonsalzen@ec.gc.ca)

© 2005 Author(s). This work is licensed under a Creative Commons License.

Title Page

Abstract

Introduction

Conclusions

References

Tables

Figures

◀

▶

◀

▶

Back

Close

Full Screen / Esc

Print Version

Interactive Discussion

EGU

Abstract

An efficient and accurate method for the representation of particle size distributions in atmospheric models is proposed. The method can be applied, but is not necessarily restricted, to aerosol mass and number size distributions. A piecewise log-normal approximation of the number size distribution within sections of the particle size spectrum is used. Two of the free parameters of the log-normal approximation are obtained from the integrated number and mass concentration in each section. A third parameter is prescribed. The method is efficient in a sense that only relatively few calculations are required for applications of the method in atmospheric models.

Applications of the method to observed size distributions and simulations of nucleation, condensation, gravitational settling, and wet deposition with a single column model are described. The accuracy of the method is considerably higher than the accuracy of the frequently used bin method in these tests.

1. Introduction

Models such as atmospheric general circulation models (AGCMs) and air quality models often lack the ability to predict aerosol size distributions mainly because of the large computational costs that are associated with a prognostic treatment of aerosol dynamical processes. Instead, parameterizations of aerosol chemical and physical processes are commonly based on highly idealized size distributions, for example, with constant size parameters. However, aerosol size distributions are considerably variable over a wide range of spatial and temporal scales in the atmosphere (Gilliani et al., 1995; von Salzen et al., 2000; Birmili et al., 2001). Unaccounted variability in size distributions is a primary source of uncertainty in studies of aerosol effects on clouds and climate (e.g. Feingold, 2003).

Consequently, accurate and computationally efficient numerical methods are required for the representation of aerosol size distributions in aerosol models.

Piecewise log-normal approximation

K. von Salzen

Title Page

Abstract

Introduction

Conclusions

References

Tables

Figures

◀

▶

◀

▶

Back

Close

Full Screen / Esc

Print Version

Interactive Discussion

Observed aerosol number size distributions can often be well approximated by a series of overlapping modes, with the size distribution for each mode represented by the log-normal distribution, i.e.,

$$n(R_p) = \frac{dN}{d \ln (R_p/R_0)} = \frac{N}{\sqrt{2\pi} \ln \sigma} \exp \left\{ -\frac{[\ln (R_p/R_0) - \ln (R_g/R_0)]^2}{2 \ln^2 \sigma} \right\},$$

with particle radius R_p , mode mean particle radius R_g , total number of particles per unit volume (or mass) N , and geometric standard deviation σ (e.g. Whitby, 1978; Seinfeld and Pandis, 1998; Remer et al., 1999). R_0 is an arbitrary reference radius (e.g. 1 μm) that is required for a dimensionally correct formulation.

The so-called modal approach in aerosol modelling is based on the idea that aerosol size distributions can be approximated using statistical moments with idealized properties (Whitby, 1981; Binkowski and Shankar, 1995; Whitby, 1997; Wilck and Stratmann, 1997; Ackermann et al., 1998; Harrington and Kreidenweis, 1998; Wilson et al., 2001). Typically, a number of overlapping log-normally distributed modes (e.g. for nucleation, accumulation and coarse mode) are assumed to account for different types of aerosols and processes in the atmosphere. An important variant of the modal approach is the quadrature method of moments, QMOM (McGraw, 1997; Wright et al., 2001; Yu et al., 2003), which is not necessarily constrained to log-normally distributed modes.

In practice, the log-normal distribution often yields good approximations of size distributions with clearly distinct modes under ideal conditions. However, it has been recognized that non-linear dynamical processes, such as aerosol activation and condensation, can lead to substantially skewed or even discontinuous size distributions (e.g. Kerminen and Wexler, 1995; Gilliani et al., 1995; von Salzen and Schlünzen, 1999b; Zhang et al., 2002).

Size distributions with non-ideal features can be well approximated with the bin approach, also often called “sectional” or “discrete” approach (Gelbard and Seinfeld, 1980; Warren and Seinfeld, 1985; Gelbard, 1990; Seigneur, 1982; Jacobson, 1997;

Piecewise log-normal approximation

K. von Salzen

Title Page

Abstract

Introduction

Conclusions

References

Tables

Figures

◀

▶

◀

▶

Back

Close

Full Screen / Esc

Print Version

Interactive Discussion

EGU

Piecewise log-normal approximationK. von Salzen

[Title Page](#)[Abstract](#)[Introduction](#)[Conclusions](#)[References](#)[Tables](#)[Figures](#)[◀](#)[▶](#)[◀](#)[▶](#)[Back](#)[Close](#)[Full Screen / Esc](#)[Print Version](#)[Interactive Discussion](#)

EGU

Lurmann et al., 1997; Russell and Seinfeld, 1998; Meng et al., 1998; von Salzen and Schlünzen, 1999a; Pilinis et al., 2000; Gong et al., 2003). According to the bin approach, a range of particle sizes is subdivided into a number of bins, or sections, with discrete values of the size distribution in each bin.

5 Several studies compared results of the modal and bin approaches based on a limited number of simulations of aerosol dynamical processes (e.g. Seigneur et al., 1986; Zhang et al., 1999; Wilson et al., 2001; Zhang et al., 2002; Korhonen et al., 2003). According to the studies, the modal approach performed well in terms of computationally efficiency and is able to reproduce important features of the size distributions. 10 However, results with this approach were noticeably biased in simulations of coagulation and condensational growth in some of the studies. On the other hand, the bin approach produced acceptable results for a relatively large number of bins or in combination with techniques that minimize the numerical diffusivity that is associated with this approach (Lurmann et al., 1997, e.g.). Computational efficiencies were generally 15 lower for this approach compared to the modal approach.

Both approaches have certain constraints that are problematic for the development of parameterizations in models.

The bin approach is typically used in models to represent the time-evolution of aerosol mass size distributions. Aerosol number concentrations and other moments 20 of the distribution are obtained from diagnostic relationships that are based on the predicted mass size distribution. Owing to the lack of a prognostic treatment, the diagnosed quantities do not generally satisfy the continuity equation and can violate fundamental mathematical constraints, such as inequality relations and positive definiteness (Feller, 1971). These can be significant problems if an insufficient number of 25 bins is used. However, a large number of bins potentially leads to considerable computational costs. For example, simulations of advection and horizontal diffusion cause an overhead of about 4% in CPU time for each additional prognostic tracer in the current operational version of the Canadian Centre for Climate Modelling and Analysis (CC-

Piecewise log-normal approximationK. von Salzen

[Title Page](#)[Abstract](#)[Introduction](#)[Conclusions](#)[References](#)[Tables](#)[Figures](#)[◀](#)[▶](#)[◀](#)[▶](#)[Back](#)[Close](#)[Full Screen / Esc](#)[Print Version](#)[Interactive Discussion](#)

Cma) AGCM3 (McFarlane et al., 2005¹). Simulations of aerosol dynamical processes may lead to further and disproportional increases in CPU time.

A disadvantage for application of the modal approach in general atmospheric models is the need to account for varying degrees of overlap between different modes. Aerosol dynamical processes often lead to changes in overlap and shape of modes. Relatively complicated treatments of aerosol dynamical processes have been proposed to allow distinct modes to merge into a single mode, for example (e.g. Harrington and Kreidenweiss, 1998; Whitby et al., 2002).

It is argued here that certain advantages offered by the modal approach (e.g. observed aerosols are often nearly log-normally distributed in parts of the size spectrum) and the bin approach (e.g. flexibility and simplicity) can be exploited for the development of a hybrid method with considerably improved performance.

The mathematical framework of a new method that is based on a combination of the bin and the modal approach is described in Sect. 2. An application of the method to observed size distributions and in simulations with a single column model of the atmosphere are described in Sects. 3 and 4.

2. Formulation of the approximation method

2.1. Approximation of the aerosol number distribution

Without any loss of generality, an approximation of an aerosol number distribution may be expressed as a series of orthogonal functions, i.e.,

$$n(\varphi) = \sum_i n_i(\varphi), \quad (1)$$

¹McFarlane, N. A., Scinocca, J. F., Lazare, M., Versegny, D., Li, J., and Harvey, R.: The CCCma third generation atmospheric general circulation model (AGCM3), Atmosphere-Ocean, in preparation, 2005.

for the dimensionless size parameter $\varphi \equiv \ln(R_p/R_0)$.

The following set of functions in Eq. (1) is proposed:

$$n_i(\varphi) = n_{0,i} \exp \left[-\psi_i (\varphi - \varphi_{0,i})^2 \right] H(\varphi - \varphi_{i-1/2}) H(\varphi_{i+1/2} - \varphi) , \quad (2)$$

where $n_{0,i}$, ψ_i , and $\varphi_{0,i}$ are fitting parameters that determine the magnitude, width, respectively mean of the distribution (Sect. 2.2). $H(x)$ denotes the Heaviside step function, i.e.

$$H(x) = \begin{cases} 0 & \text{if } x < 0 , \\ \frac{1}{2} & \text{if } x = 0 , \\ 1 & \text{if } x > 0 . \end{cases}$$

so that $n_i=0$ outside each section i with the size range $\varphi_{i-1/2} \leq \varphi \leq \varphi_{i+1/2}$. Log-normal distributions with varying properties between sections are used as basis functions in each section (Eq. 2). Hence, Eqs. (1) and (2) define a piecewise log-normal approximation (PLA) of the aerosol number distribution.

As will be demonstrated in the following sections, Eqs. (1) and (2) can be directly used for the approximation of observed size distributions and development of parameterizations in models.

Note that similar to the traditional bin approach (e.g., which can be obtained for $\psi_i=0$), the approach in Eq. (2) ensures that $n(\varphi) \geq 0$ for any given value of φ . This is not necessarily the case for other potential prescriptions, e.g. a representation of the basis functions in terms of polynomials. Additionally, the PLA method presented here has the advantages that the method is exact for strictly log-normally distributed aerosol number concentrations and that it is straightforward to calculate any higher moment of the approximated size distribution. The latter is particularly important for potential applications of the method to the development of parameterizations. Finally, approximated size distributions generally converge to the exact solution for a sufficiently large number of sections for appropriate choices of the fitting parameters.

Piecewise log-normal approximation

K. von Salzen

Title Page

Abstract

Introduction

Conclusions

References

Tables

Figures

◀

▶

◀

▶

Back

Close

Full Screen / Esc

Print Version

Interactive Discussion

2.2. Determination of the fitting parameters

The fitting parameters $n_{0,i}$, ψ_i , and $\varphi_{0,i}$ in Eq. (2) can be obtained in various ways. Here it is proposed to prescribe one of these parameters and to calculate the other two parameters for given integrated number (N_i) and mass (M_i) concentrations in each section. This approach leads to a self-consistent representation of these quantities in numerical models and also leads to expressions that are relatively straightforward to evaluate.

First, it is useful to introduce the k th moment μ_{ki} of the size distribution in section i , i.e.

$$\mu_{ki} \equiv \int_{\varphi_{i-1/2}}^{\varphi_{i+1/2}} R^k n(\varphi) d\varphi .$$

Using Eqs. (1) and (2) it follows that

$$\mu_{ki} = R_0^k n_{0,i} I_{ki} ,$$

with

$$I_{ki} = \frac{1}{2} \sqrt{\frac{\pi}{|\psi_i|}} f_{ki} \exp \left(k\varphi_{0,i} + \frac{k^2}{4|\psi_i|} \right) ,$$

and

$$f_{ki} = \begin{cases} \operatorname{erf}(a_{ki+1/2}) - \operatorname{erf}(a_{ki-1/2}) & \text{if } \psi_i > 0 , \\ \operatorname{erfi}(a_{ki+1/2}) - \operatorname{erfi}(a_{ki-1/2}) & \text{if } \psi_i < 0 . \end{cases}$$

The arguments of the error function $\operatorname{erf}(x)$ and imaginary error function $\operatorname{erfi}(x)$ in f_{ki} are

Title Page

Abstract

Introduction

Conclusions

References

Tables

Figures

◀

▶

◀

▶

Back

Close

Full Screen / Esc

Print Version

Interactive Discussion

given by:

$$a_{ki+1/2} = -\sqrt{|\psi_i|} (\Delta\varphi_i - \Delta\varphi_*) - \frac{k \operatorname{sgn}(\psi_i)}{2\sqrt{|\psi_i|}},$$

$$a_{ki-1/2} = -\sqrt{|\psi_i|} \Delta\varphi_i - \frac{k \operatorname{sgn}(\psi_i)}{2\sqrt{|\psi_i|}},$$

with $\operatorname{sgn}(x) = 2H(x) - 1$,

$$\Delta\varphi_i \equiv \varphi_{0,i} - \varphi_{i-1/2}, \quad (3)$$

and section size $\Delta\varphi_* \equiv \varphi_{i+1/2} - \varphi_{i-1/2}$.

Consequently, the integrated number ($k=0$) and mass ($k=3$) concentrations in each section are:

$$N_i = n_{0,i} l_{0i}, \quad (4)$$

$$M_i = \frac{4\pi}{3} \rho_{p,i} R_0^3 n_{0,i} l_{3i}, \quad (5)$$

where $\rho_{p,i}$ is the particle density,

As shall be seen, it is useful for the calculation of the fitting parameters to also introduce the dimensionless size ratio

$$r_i \equiv \frac{\hat{\varphi}_i - \varphi_{i-1/2}}{\Delta\varphi_*}, \quad (6)$$

where

$$\hat{\varphi}_i \equiv \ln \left[\frac{1}{R_0} \left(\frac{3}{4\pi\rho_{p,i}} \frac{M_i}{N_i} \right)^{1/3} \right].$$

Title Page

Abstract

Introduction

Conclusions

References

Tables

Figures

◀

▶

◀

▶

Back

Close

Full Screen / Esc

Print Version

Interactive Discussion

Piecewise log-normal approximation

K. von Salzen

Title Page

Abstract

Introduction

Conclusions

References

Tables

Figures

◀

▶

◀

▶

Back

Close

Full Screen / Esc

Print Version

Interactive Discussion

EGU

is an effective particle size.

r_i (Eq. 6) characterizes the skewness of the approximated size distribution within each section. For example, consider two populations of aerosol particles that have the same total number of particles but different total mass concentrations within a given range of particle sizes. This can only be the case if the population with the higher mass concentration includes fewer of the small and more of the big particles compared to the other population. Hence, the number size distribution of the former aerosol population is skewed towards larger particle sizes relative to the other number size distribution. Any meaningful values of N_i and M_i require that $0 \leq r_i \leq 1$. Mathematically, the boundary of the manifold that contains the solutions to Eqs. (4) and (5) is given by delta-distributed particle number concentrations for minimum and maximum particle sizes in the given size range (i.e. corresponding to the section boundaries).

Combination of an expression for M_i/N_i from Eqs. (4) and (5) with Eq. (6) conveniently eliminates $n_{0,i}$, i.e.

$$\frac{f_{3i}}{f_{0i}} = \exp \left[3(r_i \Delta\varphi_* - \Delta\varphi_i) - \frac{9}{4|\psi_i|} \right]. \quad (7)$$

The only unknown parameters in this equation are $\Delta\varphi_i$ and ψ_i if N_i and M_i and the section boundaries are given. It is suggested to prescribe ψ_i so that this equation can be used to determine $\Delta\varphi_i$. Subsequently, Eq. (3) can be used to determine the value of the fitting parameter $\varphi_{0,i}$.

An example for $\Delta\varphi_i$ from the solution of Eq. (7) is shown in Fig. 1 for a section size $\Delta\varphi_* = \frac{1}{3}[\ln(1.75) - \ln(0.05)]$ (i.e. similar to the application in Sect. 3).

Note that Eq. (7) does not have any solution for $\Delta\varphi_i$ within a certain range of values of ψ_i and r_i . Therefore, ψ_i is selected such that ψ_i is equal to an arbitrarily prescribed value $\psi_{m,i}$ inside the region for which a solution of Eq. (7) exists. Outside that region, a different value than that is selected in order to ensure that a solution exists. In that

[Title Page](#)
[Abstract](#)
[Introduction](#)
[Conclusions](#)
[References](#)
[Tables](#)
[Figures](#)
[◀](#)
[▶](#)
[◀](#)
[▶](#)
[Back](#)
[Close](#)
[Full Screen / Esc](#)
[Print Version](#)
[Interactive Discussion](#)

case, ψ_j should be as close as possible to $\psi_{m,i}$. Therefore,

$$\psi_j = \begin{cases} \min(\psi_{m,i}, \psi_j) & \text{if } \psi_{m,i} < 0, \\ \max(\psi_{m,i}, \psi_j) & \text{if } \psi_{m,i} > 0, \end{cases} \quad (8)$$

where ψ_j represents a threshold for which a solution of Eq. (7) can be found (i.e. as indicated by the green line in Fig. 1). This algorithm can be applied to $0 \leq r_i \leq 1$ and $-\infty \leq \psi_{m,i} \leq \infty$ for

$$\lim_{r_i \rightarrow 0,1} \psi_j = \begin{cases} +\infty & \text{if } \psi_j > 0, \\ -\infty & \text{if } \psi_j < 0. \end{cases}$$

In practice, it should be sufficient to create a look-up table for $\Delta\varphi_j$ as a function of ψ_j and r_i and to use this result to obtain the complete set of fitting parameters from Eqs. (3) and Eq. (4) or (5). Although not necessary, it is convenient to assume that all sections have the same size so that only one look-up table is required.

The algorithm described above is summarized in Fig. 2. It provides the fitting parameters for each section in Eq. (2) for given values of the number and mass concentrations in the same section.

While the accuracy of the approximation of a size distribution in terms of log-normal size distributions according to Eq. (2) depends on the values of $\psi_{m,i}$, no attempt is made here to calculate $\psi_{m,i}$ as part of the algorithm. Tests with the method under various conditions give evidence for a relatively weak dependency of the errors of the method on $\psi_{m,i}$ within a substantial range for this parameter (e.g., Sects. 3 and 4).

The accuracy of the transformations from N_j and M_j to log-normal size distributions according to the algorithm (Fig. 2) and vice versa (Eqs. 4 and 5) depends on the accuracy of the tabulated data for $\Delta\varphi_j$. However, for typical applications, (e.g. in the examples presented in the following sections) sufficient accuracy can usually be achieved for reasonably small table sizes. If necessary, the accuracy can be additionally increased by directly solving Eq. (7) instead of (or in addition to) the table look-up step.

2.3. Computational costs of the method

For applications of the PLA method in numerical models it is useful to consider the computational costs that are potentially associated with the method. In a model, the calculations of r_i and $n_{0,i}$ in Fig. 2 would likely be the most expensive steps because of the need to evaluate the functions $\ln(x)$ and $\text{erf}(x)$ (respectively $\text{erfi}(x)$) for each section according to Eqs. (6) and (4). In comparison, the costs associated with the table look-up are relatively minor for a typical Fortran 90-implementation on an IBM pSeries 390 system with POWER4 microprocessor architecture at the Canadian Meteorological Centre (i.e. $\approx 1/3$ of the total costs of the method). These costs are considerably smaller than the costs that would typically be associated with parameterizations of bulk aerosol processes in atmospheric models.

3. Application to observed size distributions

As a first test of the PLA method, the method was used to approximate aerosol size distributions that are based on observational results from the New York City (NYC) Urban Plume Experiment that took place between 1 to 28 July 1996 (Kleinman et al., 2000). In this experiment, aerosol number size distributions were determined from an aircraft that was equipped with a Passive Cavity Aerosol Spectrometer Probe (PCASP) with 15 particle size classes in the diameter range from 0.1 to 3.5 μm . The PCASP dries the sampled aerosol by heating so that the aerosol size distributions are representative for solid aerosol particles.

The observed number size distributions were first fitted using cubic interpolating splines for each one of the 7818 samples in order to obtain continuous distributions (n_{spl}). Secondly, n_{spl} was used to calculate the corresponding mass size distribution for an arbitrary particle density of $\rho_p = 1 \text{ g cm}^{-3}$. Average results for the original data and interpolated number and mass size distributions for this experiment are shown in Fig. 3. Also shown are the results of the bin and PLA methods for 3 equally-sized

Title Page

Abstract

Introduction

Conclusions

References

Tables

Figures

◀

▶

◀

▶

Back

Close

Full Screen / Esc

Print Version

Interactive Discussion

sections for the total particle diameter range from 0.1 to 3.5 μm .

Results in Fig. 3 for the number and mass size distributions according to the bin approach (blue lines) were obtained from

$$n_{\text{bin},i} = \frac{1}{\Delta\varphi_*} \int_{\varphi_{i-1/2}}^{\varphi_{i+1/2}} n_{\text{spl}}(\varphi) d\varphi,$$
$$m_{\text{bin},i} = \frac{4\pi}{3} \frac{\rho_p}{\Delta\varphi_*} \int_{\varphi_{i-1/2}}^{\varphi_{i+1/2}} R^3 n_{\text{spl}}(\varphi) d\varphi,$$

for each section ($i=1,2,3$). As an alternative to the results for $m_{\text{bin},i}$, the mass size distribution has also been diagnosed based on the number size distribution, i.e.

$$\hat{m}_{\text{bin},i} = \frac{4\pi}{3} \rho_p R_{c,i}^3 n_{\text{bin},i},$$

where $R_{c,i}$ is the radius in the centre of the sections (green line in Fig. 3b).

For the PLA method, n_{spl} was integrated over each section to determine the number and mass concentrations which were used to obtain the fitting parameters in Eq. (2) according to the procedure described in Sect. 2.2.

Results obtained with the PLA method are much closer to the reference size distribution in comparison to the bin approach in Fig. 3. Although both approaches produce the same mean number and mass concentrations for each section (per definition), the statistical properties of the size distributions, e.g. skewness, are apparently much better captured with the PLA method (red vs. blue lines in Fig. 3). Furthermore, the bin approach leads to significantly biased results for the mass size distribution if the integrated number concentration in each section is the only available statistical information for the fit (green line in Fig. 3). This illustrates that it may be problematic to use a diagnostic relationship between aerosol number and mass size distributions in an aerosol model if the size distribution is not well resolved.

Figure 4 shows root mean square (rms) differences between the approximated and spline interpolated size distributions as a function of the number of sections. For the

Piecewise log-normal approximation

K. von Salzen

Title Page

Abstract

Introduction

Conclusions

References

Tables

Figures

◀

▶

◀

▶

Back

Close

Full Screen / Esc

Print Version

Interactive Discussion

Piecewise log-normal approximationK. von Salzen

[Title Page](#)[Abstract](#)[Introduction](#)[Conclusions](#)[References](#)[Tables](#)[Figures](#)[|◀](#)[▶|](#)[◀](#)[▶](#)[Back](#)[Close](#)[Full Screen / Esc](#)[Print Version](#)[Interactive Discussion](#)

EGU

PLA method, $\psi_{m,i}$ (Eq. 8) was determined by minimizing the rms differences (red lines, for $\psi_{m,i}=2.9, -0.2, 1.8$). Additional tests with $\psi_{m,i}=1$ (cyan lines) and $\psi_{m,i}=4$ (green lines) for all sections are also shown in the figure. The rms errors for the PLA method with the various choices for $\psi_{m,i}$ are systematically lower than those for the bin method, especially at larger number of sections. The PLA method for 3 sections produces roughly the same rms differences as the bin approach for 10 sections. When 15 sections are employed for the PLA method, about 7 times the number of sections is required to obtain the same accuracy in the bin method. Errors caused by non-optimal choices for $\psi_{m,i}=1$ for the PLA method are small compared to the errors that are associated with the bin method.

4. Single-column model simulations

As an application and further test of the PLA method, the method has been used in the development of parameterizations for particle nucleation (i.e. the formation of new particles from the gas-phase), condensation of sulphuric acid (H_2SO_4), and gravitational settling. These processes are strongly dependent upon particle size. Consequently, simulations of these processes are sensitive to the numerical representation of the particle size distribution.

The parameterizations of nucleation, condensation, and gravitational settling are described in the Appendix. The basic physical and chemical equations have been discretized using the PLA and bin methods in two different versions of the model. This allows a direct comparison of both methods. Different numerical techniques are used for both methods depending on the different information that is available about the aerosol size distribution in each method. The numerical approach that is used for the bin approach is similar to the approach that is typically used in aerosol models.

4.1. Model description

The parameterizations of nucleation, condensation, and gravitational settling have been implemented in the CCCma single column model (SCM4). This model uses the same physics and chemistry parameterizations as in CCCma's fourth generation AGCM (von Salzen et al., 2005). The aerosol concentrations, i.e. M_i for the PLA and bin approaches and N_i for the PLA approach, are carried as fully prognostic tracers in SCM4.

The model domain extends from the surface up to the stratopause region (1 hPa, approximately 50 km above the surface). This region is spanned by 35 layers. The mid point of the lowest layer is approximately 50 m above the surface at sea level. Layer depths increase monotonically with height from approximately 100 m at the surface to 3 km in the lower stratosphere. The vertical discretization is in terms of rectangular finite elements defined for a hybrid vertical coordinate as described by Laprise and Girard (1990). Although the single column model does not resolve any processes that occur in the horizontal direction, results are meant to represent the mean situation in an area similar in size to a typical AGCM grid cell, e.g. for horizontal grid sizes on the order of hundreds of kilometers.

The model time step in SCM4 is 20 min. The discretization in time is based on the leapfrog time stepping method.

In addition to the newly introduced processes, the aerosol tracers are subject to vertical transport and wet deposition in the model. For simplicity, wet deposition is treated as a size-independent process based on the parameterizations that are available for bulk sulphate aerosol in SCM4 (Lohmann et al., 1999; von Salzen et al., 2000). The diurnally varying photochemical production of H_2SO_4 is calculated at each time step for climatologically representative concentrations of the hydroxyl radical (OH) and sulphur dioxide (SO_2) from previous simulations with AGCM4.

Title Page

Abstract

Introduction

Conclusions

References

Tables

Figures

◀

▶

◀

▶

Back

Close

Full Screen / Esc

Print Version

Interactive Discussion

4.2. Experiment setup

The simulations were performed for the Southern Great Plains (SGP) site (at 36°37' N 97°30' W) of the U.S. Department of Energy Atmospheric Radiation Measurement Program (ARM). The simulation period is from 1–31 May 2003, which overlaps with the ARM May 2003 Aerosol Intensive Operations (IOP) period (e.g. Feingold et al., 2005²).

The model has been used to simulate the time evolution of the ammonium sulphate [(NH₄)₂SO₄] aerosol size distribution at the SGP site for a particle radius range from 0.05 to 1.75 μm. Different numbers of sections have been used in different simulations to test the convergence of the numerical solutions for increasing numbers of section, similar to the comparison in the previous section.

For the present study, the winds were prescribed based on hourly large-scale analysis results. Temperature and humidity in SCM4 were forced using hourly analyzed advective tendencies for temperature and humidity. Results for temperature and humidity were additionally nudged towards analyzed temperature and humidity profiles. The analysis of meteorological results is based on numerical weather prediction products with additional constraints from surface and top-of-the-atmosphere measurements (Xie et al., 2004).

Analysis results were not available for initialization or forcing of chemical tracers in the present study. Horizontal transport processes were therefore neglected in the simulations. An iterative approach was employed in order to minimize the impact of the model spin-up period on the results. The model was repeatedly integrated for the same time period. Each simulation was initialized with concentrations from a previous model integration. This procedure was repeated for a total simulation period of 5 months until the aerosol concentrations were nearly in equilibrium. Only the results of the last month

²Feingold, G., Furrer, R., Pilewskie, P., Remer, L. A., Min, Q., and Jonsson, H.: Aerosol Indirect Effect Studies at Southern Great Plains during the May 2003 Intensive Operations Period, *J. Geophys. Res.*, submitted, 30 Nov 2004.

Title Page

Abstract

Introduction

Conclusions

References

Tables

Figures

◀

▶

◀

▶

Back

Close

Full Screen / Esc

Print Version

Interactive Discussion

of the simulations were analyzed.

4.3. Results

Figure 5 shows the integrated $(\text{NH}_4)_2\text{SO}_4$ aerosol number and mass concentrations in the particle radius range 0.05 to 1.75 μm from a simulation with the PLA method with 40 sections for the aerosol number and mass concentrations ($i=1, \dots, 40$). In the simulation, the highest aerosol number concentrations occur in the upper troposphere. Favourable conditions, such as low temperatures and high relative humidities, lead to high nucleation rates at these levels (e.g. Seinfeld and Pandis, 1998). However, aerosol particles at these levels are relatively small so that very little mass is associated with these particles. The maximum in aerosol mass concentration occurs in the lower troposphere where concentrations of SO_2 are high and condensation leads to efficient growth of the particles.

The simulated concentrations are quite variable in time. Most of the variability in the concentrations arises from intermittent wet deposition events. Simulated wet deposition rates are particularly high during the time period 14–24 May (Fig. 6). A large fraction of the precipitation results from moderate and deep convection in the simulation.

Variations in the magnitudes of the sources and sinks of aerosols are also connected to variations in the sizes of the aerosol particles (Fig. 7a). A single size mode is simulated, corresponding to the particle accumulation mode in the atmosphere. The deposition of aerosols does not directly lead to any noticeable changes in particle size. However, the model typically predicts increases in particle size during the time periods following large wet deposition events. This is presumably partly caused by a reduced total aerosol surface area. Consequently, the condensation of H_2SO_4 onto the aerosol particles that have not been removed by wet deposition is more efficient compared to the time period before the event. Additionally, the reduction in total surface area leads to increased nucleation rates during the time period following large wet deposition events (see Eq. A3) which eventually leads to the re-establishment of an

Piecewise log-normal approximation

K. von Salzen

Title Page

Abstract

Introduction

Conclusions

References

Tables

Figures

◀

▶

◀

▶

Back

Close

Full Screen / Esc

Print Version

Interactive Discussion

accumulation mode that more or less resembles the mode that existed prior to the wet deposition event.

As already mentioned, the primary purpose of the simulations is to test the performance of the PLA method and to compare results from this method with results from the bin approach. Results in Fig. 7 serve as an illustration of the approach in this study.

The most accurate simulations of the aerosol processes were obtained from control simulations with a total of 80 aerosol tracers for the PLA (Fig. 7a) and the bin (Fig. 7b) method, corresponding to 40 sections for the PLA and 80 sections for the bin method. Results of the control simulations agree well with each other in terms of concentrations and sizes of the particles. However, results of the comparison in Sect. 3 indicate that the accuracy of the bin approach is systematically lower than the accuracy of the PLA method, even at these relatively large number of sections (e.g. Fig. 4). This explains why results using the bin approach are characterized by slightly weaker maxima of the aerosol mass size distribution compared to the results of the PLA method.

The accuracy of the PLA method depends only weakly on the number of sections in the simulation. Results for 3 sections (i.e. 6 tracers) with the PLA method are very similar to the results of the control simulation (Fig. 4c). The main differences are slightly weaker maxima and broader size spectra.

In contrast, there is a marked reduction in the quality of the results of the bin approach for a decreased number of sections. A simulation with 10 aerosol tracers produces much broader size distributions and therefore reveals very little about the temporal evolution in particle size as apparent in the control simulation (Fig. 4d compared to Fig. 4b). The simulated size distribution is also shifted towards much smaller particle sizes compared to the control simulation. Artifacts such as these are typical of the upstream method, which has been used for the bin approach (see Appendix A.2). This method is only first-order accurate and thus tends to produce strong numerical diffusion (e.g. Bott, 1989). The introduction of higher-order schemes may potentially lead to improvements in these results (e.g. von Salzen and Schlünzen, 1999a). However, these methods would typically only be useful for relatively well resolved size distribu-

Piecewise log-normal approximationK. von Salzen

Title Page

Abstract

Introduction

Conclusions

References

Tables

Figures

◀

▶

◀

▶

Back

Close

Full Screen / Esc

Print Version

Interactive Discussion

tions and none of them would lead to conservation of aerosol number in simulations of condensation.

Results of the bin approach for 10 sections (Fig. 4d) have an appreciably lower accuracy than the results of the PLA method for 3 sections (Fig. 4c). This gives evidence that aerosol dynamical processes lead to higher order errors than what might be expected from the basic analysis of the discretization method in Sect. 3. Comparisons in that section showed that PLA and bin methods performed about equally well at these numbers of sections.

Figure 8 shows rms differences for a number of simulations with the PLA and bin methods. Similar to Fig. 4, the accuracy of the results of the PLA and bin methods generally increases with increasing number of sections. The PLA method produces a systematically higher accuracy than the bin method. The difference in accuracy between both methods is more apparent for the aerosol number concentration than it is for the aerosol mass concentration. However, the aerosol number concentration is a purely diagnostic quantity in the context of the bin method (Eq. A5) whereas it is predicted in the simulations with the PLA method.

Similar to the conclusion in Sect. 3, the accuracy of the results with the PLA method is only weakly sensitive to the choice of $\psi_{m,i}$ (Fig. 8).

Finally, it is interesting to compare the results of the simulations in (Fig. 7) to observations at the SGP site during the ARM Aerosol IOP. An optical particle counter (OPC, Particle Measuring Systems Model PCASP-X) provided size distribution data in 31 size classes for particle diameters between 0.1 and 10 μm (Sheridan et al., 2001). The aerosol sample stream that enters the OPC is heated to a relative humidity of 40% (or less) so that the effect of aerosol water is negligible. This allows a direct comparison between the observed and simulated size distributions. For the current study, the observed aerosol number concentrations in each size class were converted into an aerosol mass size distribution based on the assumption of spherical particles with a density of 1.769 kg m^{-3} .

Observations are available for limited time periods during the IOP. Hourly average

Piecewise log-normal approximationK. von Salzen

[Title Page](#)[Abstract](#)[Introduction](#)[Conclusions](#)[References](#)[Tables](#)[Figures](#)[◀](#)[▶](#)[◀](#)[▶](#)[Back](#)[Close](#)[Full Screen / Esc](#)[Print Version](#)[Interactive Discussion](#)

results for these time periods are shown in Fig. 9.

Similar to the simulations (Fig. 7), a single particle mode has been observed in the range from 0.1 to 1 μm . Also, the maxima in the aerosol size distribution occur at similar particle sizes. However, the observed size distributions are considerably broader and more variable. It is likely that at least part of the differences are caused by the omission of horizontal transport of aerosols. Other likely causes are the omission of aerosol in-cloud production, coagulation, contributions of non-sulphate aerosols, as well the simplified treatments of wet deposition and photochemical production of H_2SO_4 in the simulations. Although the parameterized physics is incomplete, the results in Fig. 8 give evidence that the PLA method provides a much more accurate and efficient platform for aerosol modelling than the bin method.

5. Conclusions

Aerosol physical and chemical processes generally depend on aerosol number, mass, and other moments of the aerosol size distribution. Currently, models typically predict aerosol mass or number based on numerical approaches that do not guarantee continuity of these quantities at the same time. Additionally, considerable computational costs are often incurred from traditional treatments of aerosol dynamical processes for sufficiently accurate results.

The piecewise log-normal approximation method (PLA) that is proposed here addresses these concerns by combining a sectional representation of the size distribution with an analytical description of the size distribution. The basic idea is that a sectional treatment is appropriate for large particle size scales (i.e. $\delta\varphi > \Delta\varphi_*$). However, unresolved features of the size distribution on smaller scales (i.e. $\delta\varphi < \Delta\varphi_*$) may be approximated in terms of analytical basis functions within each section. The advantage of log-normal basis functions is that a wide range of conditions can be described and that it is straightforward to obtain any desired statistical moment of the distribution. The latter is particularly important for applications of the PLA method to the development of

Piecewise log-normal approximation

K. von Salzen

Title Page

Abstract

Introduction

Conclusions

References

Tables

Figures

◀

▶

◀

▶

Back

Close

Full Screen / Esc

Print Version

Interactive Discussion

parameterizations.

A computationally efficient method is proposed to compute two of the free parameters of the log-normal basis functions from the number and mass concentrations in each section. A third parameter is taken to be constant. Although it should in principle be possible to optimally specify the third parameter, this study gives evidence for a relatively weak dependency of the results of the method on the value of this parameter.

An application of the PLA method to the approximation of observed size distributions gives evidence for high accuracy of the method for a wide range of the number of sections. In this example, results of the PLA method are at least as accurate as the results of the traditional bin approach for a three times larger number of sections in the bin approach.

Differences between the accuracies of the PLA and bin methods are even more apparent in applications of the methods to prognostic simulations with a single column model. The processes included in these simulations are vertical transport, nucleation, condensation, gravitational settling, and wet deposition for ammonium sulphate aerosol.

In the future, the PLA method will also be applied to the development of parameterizations of in-cloud aerosol production and coagulation of sulphate and non-sulphate aerosols. These parameterizations will be subsequently implemented into the CCCma Atmospheric General Circulation Model and tested.

A: Parameterization of nucleation and condensation

The growth of aerosol particles due to condensation of sulphuric acid (H_2SO_4) and ammonia (NH_3) can be expressed using Fick's law (e.g. Seinfeld and Pandis, 1998). NH_3 is typically highly abundant in the troposphere (e.g. Dentener and Crutzen, 1994). Hence, it can be safely assumed that condensation of NH_3 leads to nearly immediate and complete reaction of H_2SO_4 to $(\text{NH}_4)_2\text{SO}_4$ in the particles. Furthermore, the concentration of H_2SO_4 is approximately nil at the surface of the particles. This appears

Piecewise log-normal approximation

K. von Salzen

Title Page

Abstract

Introduction

Conclusions

References

Tables

Figures

◀

▶

◀

▶

Back

Close

Full Screen / Esc

Print Version

Interactive Discussion

to be a good approximation owing to the very low volatility of H_2SO_4 . Under these assumptions, the time evolution of the particle radius R_{pd} for dry (i.e. solid) aerosol can be expressed by

$$\frac{dR_{pd}}{dt} = \frac{c_g C}{R_{pd}}, \quad (\text{A1})$$

with the concentration C of H_2SO_4 (in kg m^{-3}) and

$$c_g = \left(\frac{M_{(\text{NH}_4)_2\text{SO}_4}}{M_{\text{H}_2\text{SO}_4}} \right) \frac{D F A e^{\Delta\varphi_w}}{\rho_{pd}}.$$

$M_{(\text{NH}_4)_2\text{SO}_4}$ and $M_{\text{H}_2\text{SO}_4}$ refer to the molecular weights of $(\text{NH}_4)_2\text{SO}_4$ and H_2SO_4 (in kg mol^{-1}). ρ_{pd} denotes the density of the dry aerosol (in kg m^{-3}). D represents the diffusivity of H_2SO_4 in air (in $\text{m}^2 \text{s}^{-1}$). F and A are dimensionless and size-dependent factors which account for non-continuum effects and imperfect surface accommodation (von Salzen et al., 2000). Note that unity is used for the mass accommodation coefficient in A in this study. This value appears to be in qualitatively good agreement with results of recent theoretical and laboratory studies (Kulmala and Wagner, 2001). Finally, $\Delta\varphi_w$ refers to the difference between wet and dry particle size owing to the aerosol water content, i.e.

$$\Delta\varphi_w = \ln \left(\frac{R_{pw}}{R_{pd}} \right), \quad (\text{A2})$$

for dry and wet particle radii, R_{pd} and R_{pw} . In this study, $\Delta\varphi_w$ has been determined from thermodynamic equilibrium for mean concentrations in each section (Gong et al., 2003).

Title Page

Abstract

Introduction

Conclusions

References

Tables

Figures

◀

▶

◀

▶

Back

Close

Full Screen / Esc

Print Version

Interactive Discussion

The time evolution of the H_2SO_4 concentration due to gas-phase production, nucleation, and condensation can be described by:

$$\frac{dC}{dt} = P - kC^s - 4\pi CD \sum_i \int_{\varphi_{i-1/2}}^{\varphi_{i+1/2}} F A R_{pw} n(\varphi) d\varphi. \quad (\text{A3})$$

In Eq. (A3), P represents the production of H_2SO_4 from oxidation of sulphur dioxide by the hydroxyl radical (Stockwell and Calvert, 1983). The following term represents the losses from binary homogeneous nucleation for H_2SO_4 and water vapour, with temperature and humidity dependent parameters k and s (e.g. von Salzen et al., 2000).

The last term in Eq. (A3) represents the condensation of H_2SO_4 . It follows from Eq. (A1) from integration over the size distribution. R_{pw} is calculated from $\Delta\varphi_w$ and the dry particle size $R_{pd} = R_0 \exp(\varphi)$ (Eq. A2). Note that the number size distribution in the integral in Eq. (A3) is a function of the dry particle size with constant section boundaries $\varphi_{i\pm 1/2}$. This approach is sometimes used in aerosol models to increase the numerical accuracy of simulations with varying aerosol water contents. With this approach, the concentrations of the total aerosol (including water) can be easily diagnosed based on the results for the size distribution for dry particles and Eq. (A2).

Sensitivity tests give evidence for rapid adjustment of C toward equilibrium for a wide range of atmospheric conditions that exist in large-scale atmospheric models. On the other hand, changes of P , k , s , D , F , A , $\Delta\varphi_w$, and $n(\varphi)$ are typically much smaller compared to changes in C over a model time step ($\Delta t \approx 30$ min). Hence, Eq. (A3) is integrated under the assumption of a constant aerosol size distribution during the time step.

Title Page

Abstract

Introduction

Conclusions

References

Tables

Figures

◀

▶

◀

▶

Back

Close

Full Screen / Esc

Print Version

Interactive Discussion

A.1: Application of PLA method

In order to simplify the numerical approach for the PLA method, the size-dependence of the term FA in Eqs. (A3) and (A1) is approximated by

$$FA \approx (FA)_{i-1/2} + \frac{(FA)_{i+1/2} - (FA)_{i-1/2}}{e^{\varphi_{i+1/2}} - e^{\varphi_{i-1/2}}} (e^{\varphi} - e^{\varphi_{i-1/2}})$$

for $\varphi_{i-1/2} \leq \varphi \leq \varphi_{i+1/2}$.

Equation (A1) is used to obtain a linearized expression for the change in dry particle radius during a single model time step, i.e.

$$R_{pd}(t_0 + \Delta t) = R_{pd}(t_0) + \frac{c_g(t_0)}{R_{pd}(t_0)} \int_{t_0}^{t_0 + \Delta t} C dt, \quad (\text{A4})$$

where the integral results from integration of Eq. (A3) as described in the previous section. This procedure ensures that the change in particle mass from condensation of H_2SO_4 matches the change in H_2SO_4 concentration from integration of Eq. (A3).

Calculations for each section according to Eq. (A4) are followed by a remapping procedure so that the section boundaries for dry particles remain unchanged at each time step in the model. The remapping procedure is a straightforward integration over the size distribution for the particle radii after condensation (Eq. A4), based on Eqs. (4) and (5).

For the treatment of nucleation it is assumed that the size distribution of the freshly produced particles is a delta-function for a particle size corresponding to the size of the smallest particles in the first section $i=1$. The amount of those particles is determined from integration of the nucleation term in Eq. (A3) over Δt .

Title Page

Abstract

Introduction

Conclusions

References

Tables

Figures

◀

▶

◀

▶

Back

Close

Full Screen / Esc

Print Version

Interactive Discussion

A.2: Application of bin approach

For the application of the bin approach, it is assumed that the number size distribution within each section can be approximated by

$$n(\varphi) \approx \frac{N_i}{\Delta\varphi_*},$$

for $\varphi_{i-1/2} \leq \varphi \leq \varphi_{i+1/2}$, with

$$N_i \approx \frac{M_i}{\frac{4\pi}{3} \rho_{pd} R_0^3 \exp(3\varphi_{c,i})}, \quad (\text{A5})$$

and

$$\varphi_{c,i} = \varphi_{i-1/2} + \frac{1}{2} \Delta\varphi_*. \quad (\text{A6})$$

It is further assumed that

$$FAR_{pw} \approx (FAR_{pw})_{i-1/2} + \frac{(FAR_{pw})_{i+1/2} - (FAR_{pw})_{i-1/2}}{e^{\varphi_{i+1/2}} - e^{\varphi_{i-1/2}}} (e^\varphi - e^{\varphi_{i-1/2}})$$

for $\varphi_{i-1/2} \leq \varphi \leq \varphi_{i+1/2}$.

Similar to the application of the PLA method, Eq. (A3) is integrated to obtain the change ΔC in H_2SO_4 concentration over Δt . Let ΔC_{cnd} be the contribution of condensation (i.e. from last term in Eq. A3) to ΔC . Mass continuity then implies that the aerosol mass changes according to

$$\Delta M_i = - \left(\frac{M_{(\text{NH}_4)_2\text{SO}_4}}{M_{\text{H}_2\text{SO}_4}} \right) \Delta C_{\text{cnd}}.$$

Title Page

Abstract

Introduction

Conclusions

References

Tables

Figures

◀

▶

◀

▶

Back

Close

Full Screen / Esc

Print Version

Interactive Discussion

for particles with $\varphi_{i-1/2} \leq \varphi \leq \varphi_{i+1/2}$ at the beginning of the time step. A change in aerosol mass from condensation is accompanied by a change in particle size $\Delta\varphi_{c,i}$. $\Delta\varphi_{c,i}$ can be obtained from Eq. (A5) under the assumption that $N_i = \text{const.}$:

$$\Delta\varphi_{c,i} = \frac{1}{3} \ln \left(1 + \frac{\Delta M_i}{M_i} \right).$$

On the other hand, section boundaries are not allowed to change between time steps, similar to the application of the PLA method. This requires a redistribution of mass between different sections. Hence, the mass concentration at time $t = t_0 + \Delta t$ is calculated from

$$\mathbf{M}(t_0 + \Delta t) = \mathbf{T} [\mathbf{M}(t_0) + \Delta\mathbf{M}],$$

where \mathbf{M} and $\Delta\mathbf{M}$ are vectors with elements M_j , respectively ΔM_j . \mathbf{T} is a matrix with elements

$$t_{ij} = H \left(\Delta\varphi_{(i-1/2)j}^- \right) H \left(\Delta\varphi_{(i-1/2)j}^+ \right) \frac{\Delta\varphi_{(i-1/2)j}^+}{\Delta\varphi_*} \\ + H \left(\Delta\varphi_{(i+1/2)j}^- \right) H \left(\Delta\varphi_{(i+1/2)j}^+ \right) \frac{\Delta\varphi_{(i+1/2)j}^-}{\Delta\varphi_*},$$

with

$$\Delta\varphi_{(i\pm 1/2)j}^- = \varphi_{t,(i\pm 1/2)j} - \varphi_{j-1/2},$$

$$\Delta\varphi_{(i\pm 1/2)j}^+ = \varphi_{j+1/2} - \varphi_{t,(i\pm 1/2)j},$$

and

$$\varphi_{t,(i\pm 1/2)j} = \varphi_{i\pm 1/2} - \Delta\varphi_{c,j}.$$

Aerosol mass resulting from nucleation is inserted into the first section according to the change in H_2SO_4 concentration from nucleation over Δt (Eq. A3).

Piecewise log-normal approximation

K. von Salzen

Title Page

Abstract

Introduction

Conclusions

References

Tables

Figures

◀

▶

◀

▶

Back

Close

Full Screen / Esc

Print Version

Interactive Discussion

EGU

B: Parameterization of gravitational settling

The terminal settling velocity of a spherical aerosol particle is

$$v_t = \frac{2 R_{pw}^2 \rho_{pw} g C_c}{9 \mu}, \quad (\text{B1})$$

with the gravitational acceleration g , density of the wet aerosol ρ_{pw} , and slip correction factor

$$C_c = 1 + \frac{\lambda}{R_{pw}} \left[1.257 + 0.4 \exp\left(-\frac{1.1 R_{pw}}{\lambda}\right) \right], \quad (\text{B2})$$

and mean free path of air λ (Seinfeld and Pandis, 1998).

In order to simplify the discretization and increase the efficiency of the numerical solution, the approximation

$$\exp\left(-\frac{1.1 R_{pw}}{\lambda}\right) \approx \exp\left(-\frac{1.1 R_0 e^{\varphi_{c,i} + \Delta\varphi_w}}{\lambda}\right)$$

is used for $\varphi_{i-1/2} \leq \varphi \leq \varphi_{i+1/2}$ in Eq. (B2), with $\varphi_{c,i}$ from Eq. (A6).

B.1: Application of PLA method

Equation (B1) is used to calculate effective terminal settling velocities for particle number ($v_{tn,i}$) and mass ($v_{tm,i}$) in each section i from integration over the section, i.e.

$$v_{tn,i} = \frac{1}{N_i} \int_{\varphi_{w,i-1/2}}^{\varphi_{w,i+1/2}} v_t n(\varphi - \Delta\varphi_w) d\varphi,$$

$$v_{tm,i} = \frac{1}{M_i} \frac{4\pi}{3} \rho_{p,i} R_0^3 \int_{\varphi_{w,i-1/2}}^{\varphi_{w,i+1/2}} v_t e^{3\varphi} n(\varphi - \Delta\varphi_w) d\varphi,$$

5 with $\varphi_{w,i\pm 1/2} = \varphi_{i\pm 1/2} + \Delta\varphi_w$.

Piecewise log-normal approximation

K. von Salzen

Title Page

Abstract

Introduction

Conclusions

References

Tables

Figures

◀

▶

◀

▶

Back

Close

Full Screen / Esc

Print Version

Interactive Discussion

EGU

B.2: Application of bin approach

Effective terminal settling velocities are obtained for M_j from Eq. (B1) for $R_{pw} = R_0 \exp(\varphi_{c,i} + \Delta\varphi_w)$.

Acknowledgements. The author thanks S. Xie for providing the single column model forcing data and colleagues N. McFarlane, W. Merryfield, and J. Scinocca for discussions. This research was partially supported by the Climate Change Action Fund (CCAF) and the Meteorological Service of Canada.

References

- Ackermann, I. J., Hass, H., Memmesheimer, M., Ebel, A., Binkowski, F. S., and Shankar, U.: Modal aerosol dynamics model for Europe: Development and first applications, *Atmos. Environ.*, 32, 2981–2999, 1998. [3961](#)
- Binkowski, F. S. and Shankar, U.: The regional particulate matter model 1. Model description and preliminary results, *J. Geophys. Res.*, 100, 21 191–21 209, 1995. [3961](#)
- Birmili, W., Wiedensohler, A., Heintzenberg, J., and Lehmann, K.: Atmospheric particle number size distribution in central Europe: Statistical relations to air masses and meteorology, *J. Geophys. Res.*, 106, 32 005–32 018, 2001. [3960](#)
- Bott, A.: A positive definite advection scheme obtained by nonlinear renormalization of the advective fluxes, *Mon. Weather Rev.*, 117, 1006–1015, 1989. [3975](#)
- Dentener, F. and Crutzen, P. J.: A 3-dimensional model of the global ammonia cycle, *J. Atmos. Chem.*, 19, 331–369, 1994. [3978](#)
- Feingold, G.: Modeling of the first indirect effect: Analysis of measurement requirements, *Geophys. Res. Lett.*, 30, doi:10.1029/2003GL017967, 2003. [3960](#)
- Feller, W.: An introduction to probability theory and its applications, Wiley, New York, 1971. [3962](#)
- Gelbard, F.: Modeling multicomponent aerosol particle growth by vapor condensation, *Aerosol Sci. Technol.*, 12, 399–412, 1990. [3961](#)
- Gelbard, F. and Seinfeld, J. H.: Simulation of multicomponent aerosol dynamics, *J. Colloid Interface Sci.*, 78, 485–501, 1980. [3961](#)

Piecewise log-normal approximation

K. von Salzen

Title Page

Abstract

Introduction

Conclusions

References

Tables

Figures

◀

▶

◀

▶

Back

Close

Full Screen / Esc

Print Version

Interactive Discussion

Piecewise log-normal approximationK. von Salzen

[Title Page](#)[Abstract](#)[Introduction](#)[Conclusions](#)[References](#)[Tables](#)[Figures](#)[◀](#)[▶](#)[◀](#)[▶](#)[Back](#)[Close](#)[Full Screen / Esc](#)[Print Version](#)[Interactive Discussion](#)

EGU

- Gilliani, N. V., Schwartz, S. E., Leaitch, W. R., Strapp, J. W., and Isaac, G. A.: Field observations in continental stratiform clouds: Partitioning of cloud particles between droplets and unactivated interstitial aerosols, *J. Geophys. Res.*, 100, 18 687–18 706, 1995. [3960](#), [3961](#)
- 5 Gong, S. L., Barrie, L. A., Blanchet, J.-P., von Salzen, K., Lohmann, U., Lesins, G., Spacek, L., Zhang, L. M., Girard, E., Lin, H., Leaitch, R., Leighton, H., Chylek, P., and Huang, P.: Canadian Aerosol Module: A size-segregated simulation of atmospheric aerosol processes for climate and air quality models – 1. Module development, *J. Geophys. Res.*, 108, doi:10.1029/2001JD002002, 2003. [3962](#), [3979](#)
- Harrington, D. Y. and Kreidenweis, S. M.: Simulations of sulfate aerosol dynamics – Part II. Model intercomparison, *Atmos. Environ.*, 32, 1701–1709, 1998. [3961](#), [3963](#)
- 10 Jacobson, M. Z.: Development and application of a new air pollution modeling system 2. Aerosol module structure and design, *Atmos. Environ.*, 31, 131–144, 1997. [3961](#)
- Kerminen, V.-M. and Wexler, A. S.: Growth laws for atmospheric aerosol particles: An examination of the bimodality of the accumulation mode, *Atmos. Environ.*, 29, 3263–3275, 1995. [3961](#)
- 15 Kleinman, L. I., Daum, P. H., Imre, D. G., Lee, J. H., Lee, Y.-N., Nunnermacker, L. J., Springston, S. R., Weinstein-Lloyd, J., and Newman, L.: Ozone production in the New York city urban plume, *J. Geophys. Res.*, 105, 14 495–14 511, 2000. [3969](#)
- Korhonen, H., Lehtinen, K. E. J., Pirjola, L., Napari, I., and Vehkamäki, H.: Simulation of atmospheric nucleation mode: A comparison of nucleation models and size distribution representations, *J. Geophys. Res.*, 108, doi:10.1029/2002JD003305, 2003. [3962](#)
- 20 Kulmala, M. and Wagner, P. E.: Mass accommodation and uptake coefficients – a quantitative comparison, *J. Aerosol Sci.*, 32, 833–841, 2001. [3979](#)
- Laprise, R. and Girard, E.: A spectral general circulation model using a piecewise-constant finite element representation on a hybrid vertical coordinate system, *J. Climate*, 3, 32–52, 1990. [3972](#)
- 25 Lohmann, U., von Salzen, K., McFarlane, N., Leighton, H. G., and Feichter, J.: Tropospheric sulphur cycle in the Canadian general circulation model, *J. Geophys. Res.*, 104, 26 833–26 858, 1999. [3972](#)
- 30 Lurmann, F. W., Wexler, A. S., Pandis, S. N., Musarra, S., Kumar, N., and Seinfeld, J. H.: Modelling urban and regional aerosols – II. Application to California’s south coast air basin, *Atmos. Environ.*, 31, 2695–2715, 1997.

Piecewise log-normal approximationK. von Salzen

Title Page

Abstract

Introduction

Conclusions

References

Tables

Figures

◀

▶

◀

▶

Back

Close

Full Screen / Esc

Print Version

Interactive Discussion

- McGraw, R.: Description of aerosol dynamics by the quadrature method of moments, *Aerosol Sci. Technol.*, 27, 255–265, 1997. [3962](#) [3961](#)
- Meng, Z. Y., Dabdub, D., and Seinfeld, J. H.: Size-resolved and chemically resolved model of atmospheric aerosol dynamics, *J. Geophys. Res.*, 103, 3419–3435, 1998. [3962](#)
- 5 Pilinis, C., Capaldo, K. P., Nenes, A., and Pandis, S. N.: MADM – A new multicomponent aerosol dynamics model, *Aerosol Sci. Technol.*, 32, 482–502, 2000. [3962](#)
- Remer, L. A., Kaufman, Y. J., and Holben, B. N.: Interannual variation of ambient aerosol characteristics on the east coast of the United States, *J. Geophys. Res.*, 104, 2223–2231, 1999. [3961](#)
- 10 Russell, L. M. and Seinfeld, J. H.: Size- and composition-resolved externally mixed aerosol model, *Aerosol Sci. Technol.*, 28, 403–416, 1998. [3962](#)
- Seigneur, C.: A model of sulfate aerosol dynamics in atmospheric plumes, *Atmos. Environ.*, 16, 2207–2228, 1982. [3961](#)
- Seigneur, C., Hudischewskyi, A. B., Seinfeld, J. H., Whitby, K. T., Whitby, E. R., Brock, J. R., and Barnes, H. M.: Simulation of aerosol dynamics: A comparative review of mathematical models, *Aerosol Sci. Technol.*, 5, 205–222, 1986. [3962](#)
- 15 Seinfeld, J. H. and Pandis, S. N.: Atmospheric chemistry and physics: From air pollution to climate change, Wiley, New York, 1998. [3961](#), [3974](#), [3978](#), [3984](#)
- Sheridan, P. J., Delene, D. J., and Ogren, J. A.: Four years of continuous surface aerosol measurements from the Department of Energy's Atmospheric Radiation Measurement Program Southern Great Plains Cloud and Radiation Testbed site, *J. Geophys. Res.*, 106, 20 735–20 747, 2001. [3976](#)
- 20 Stockwell, W. R. and Calvert, J. G.: The mechanism of HO-SO₂ reaction, *Atmos. Environ.*, 17, 2231–2235, 1983. [3980](#)
- 25 von Salzen, K. and Schlünzen, K. H.: A prognostic physico-chemical model of secondary and marine inorganic multicomponent aerosols I. Model description, *Atmos. Environ.*, 33, 767–576, 1999a. [3962](#), [3975](#)
- von Salzen, K. and Schlünzen, K. H.: A prognostic physico-chemical model of secondary and marine inorganic multicomponent aerosols II. Model tests, *Atmos. Environ.*, 33, 1543–1552, 1999b. [3961](#)
- 30 von Salzen, K., Leighton, H. G., Ariya, P. A., Barrie, L. A., Gong, S. L., Blanchet, J.-P., Spacek, L., Lohmann, U., and Kleinman, L. I.: Sensitivity of sulphate aerosol size distributions and CCN concentrations over North America to SO_x emissions and H₂O₂ concentrations, *J. Geo-*

Piecewise log-normal approximationK. von Salzen

Title Page

Abstract

Introduction

Conclusions

References

Tables

Figures

◀

▶

◀

▶

Back

Close

Full Screen / Esc

Print Version

Interactive Discussion

phys. Res., 105, 9741–9765, 2000. [3960](#), [3972](#), [3979](#), [3980](#)

von Salzen, K., McFarlane, N. A., and Lazare, M.: The role of shallow convection in the water and energy cycles of the atmosphere, *Climate Dyn.*, in press, 2005. [3972](#)

Warren, D. R. and Seinfeld, J. H.: Simulation of aerosol size distribution evolution in systems with simultaneous nucleation, condensation, and coagulation, *Aerosol Sci. Technol.*, 4, 31–43, 1985. [3961](#)

Whitby, E., Stratmann, F., and Wilck, M.: Merging and remapping modes in modal aerosol dynamics models: A “Dynamic Mode Manager”, *J. Aerosol Sci.*, 33, 623–645, 2002. [3963](#)

Whitby, E. R.: Modal aerosol dynamics modeling, *Aerosol Sci. Technol.*, 27, 673–688, 1997. [3961](#)

Whitby, K. T.: The physical characteristics of sulfur aerosols, *Atmos. Environ.*, 12, 135–159, 1978. [3961](#)

Whitby, K. T.: Determination of aerosol growth rates in the atmosphere using lumped aerosol dynamics, *J. Aerosol Sci.*, 12, 174–178, 1981. [3961](#)

Wilck, M. and Stratmann, F.: A 2-D multicomponent modal aerosol model and its application to laminar flow reactors, *J. Aerosol Sci.*, 28, 959–972, 1997. [3961](#)

Wilson, J., Cuvelier, C., and Raes, F.: A modeling study of global mixed aerosol fields, *J. Geophys. Res.*, 106, 34 081–34 108, 2001. [3961](#), [3962](#)

Wright, D. L., Kasibhatla, P. S., McGraw, R., and Schwartz, S. E.: Description and evaluation of a six-moment aerosol microphysical module for use in atmospheric chemical transport models, *J. Geophys. Res.*, 106, 20 275–20 291, 2001. [3961](#)

Xie, S., Cederwall, R. T., and Zhang, M.: Developing long-term single-column model/cloud system-resolving model forcing data using numerical weather prediction products constrained by surface and top of the atmosphere observations, *J. Geophys. Res.*, 109, doi:10.1029/2003JD004045, 2004. [3973](#)

Yu, S., Kasibhatla, P. S., Wright, D. L., Schwartz, S. E., and McGraw, R.: Moment-based simulation of microphysical properties of sulfate aerosols in the eastern United States: Model description, evaluation, and regional analysis, *J. Geophys. Res.*, 108, doi:10.1029/2002JD002890, 2003. [3961](#)

Zhang, Y., Seigneur, C., Seinfeld, J. H., Jacobson, M. Z., and Binkowski, F. S.: Simulation of aerosol dynamics: A comparative review of algorithms used in air quality models, *Aerosol Sci. Technol.*, 31, 487–514, 1999.

Zhang, Y., Easter, R. C., Ghan, S. J., and Abdul-Razzak, H.: Impact of aerosol size representations on modeling aerosol-cloud interactions, *J. Geophys. Res.*, 107, doi:10.1029/2001JD001549, 2002. [3962](#) [3961](#), [3962](#)

ACPD

5, 3959–3998, 2005

Piecewise log-normal approximation

K. von Salzen

Title Page

Abstract

Introduction

Conclusions

References

Tables

Figures

◀

▶

◀

▶

Back

Close

Full Screen / Esc

Print Version

Interactive Discussion

EGU

Piecewise log-normal approximation

K. von Salzen

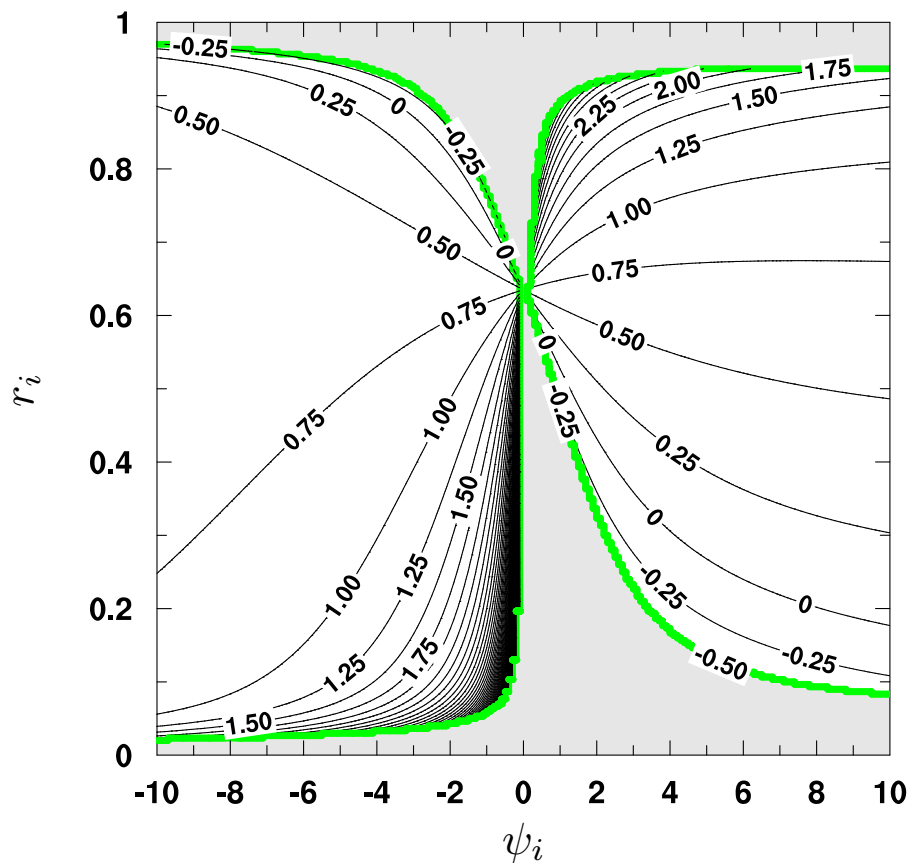


Fig. 1. $\Delta\varphi_i$ (Eq. 3) according to Eq. (7). No solution exists in the shaded area.

Title Page

Abstract

Introduction

Conclusions

References

Tables

Figures

◀

▶

◀

▶

Back

Close

Full Screen / Esc

Print Version

Interactive Discussion

EGU

Piecewise log-normal approximation

K. von Salzen

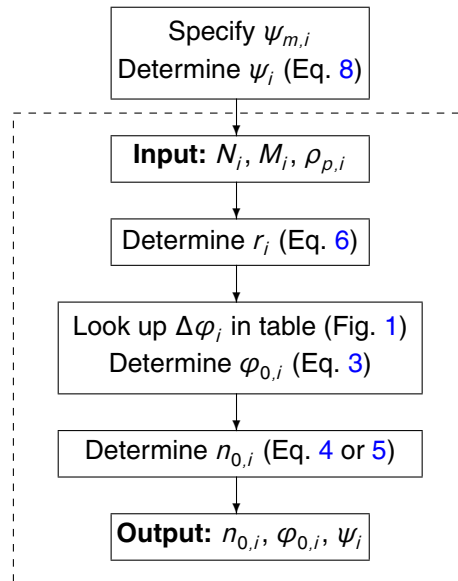


Fig. 2. Summary of the algorithm to determine the fitting parameters in Eq. (2). In applications of the algorithm in models, the steps in the box at the top should be part of the pre-processing stage in the model. The inputs for the other steps may change at each time step in the model and will generally have to be repeated once size distributions are updated in the model.

Title Page

Abstract

Introduction

Conclusions

References

Tables

Figures

◀

▶

◀

▶

Back

Close

Full Screen / Esc

Print Version

Interactive Discussion

EGU

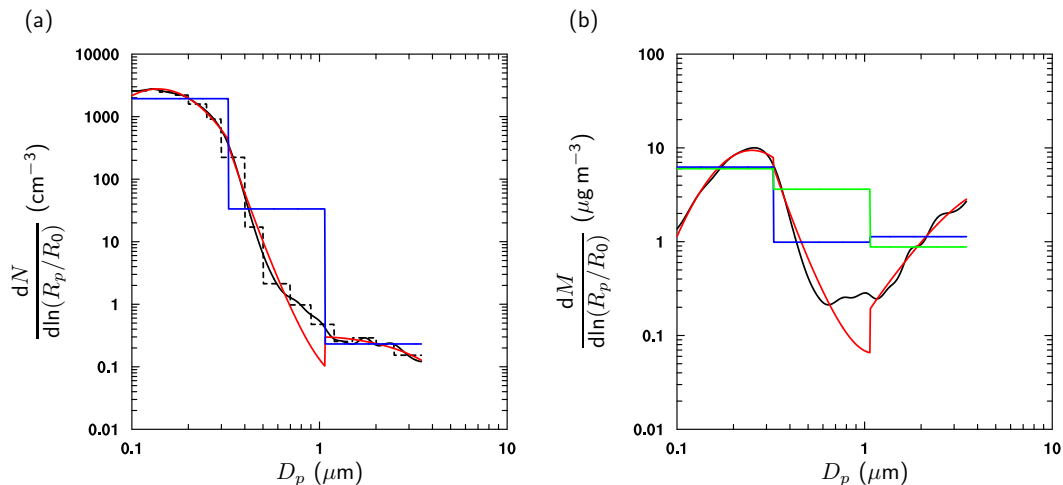


Fig. 3. Average observed (dashed line) and interpolated size distributions (full black lines) for aerosol number **(a)** and mass **(b)** for all samples during the NYC Urban Plume Experiment. Blue lines refer to the corresponding approximated results based on the bin approach, red lines to the PLA method for 3 sections. The green line in (b) is for a diagnosed size distribution based on results of the bin method in (a) as described in the text.

Piecewise log-normal approximation

K. von Salzen

Title Page

Abstract

Introduction

Conclusions

References

Tables

Figures

◀

▶

◀

▶

Back

Close

Full Screen / Esc

Print Version

Interactive Discussion

EGU

Piecewise log-normal approximation

K. von Salzen

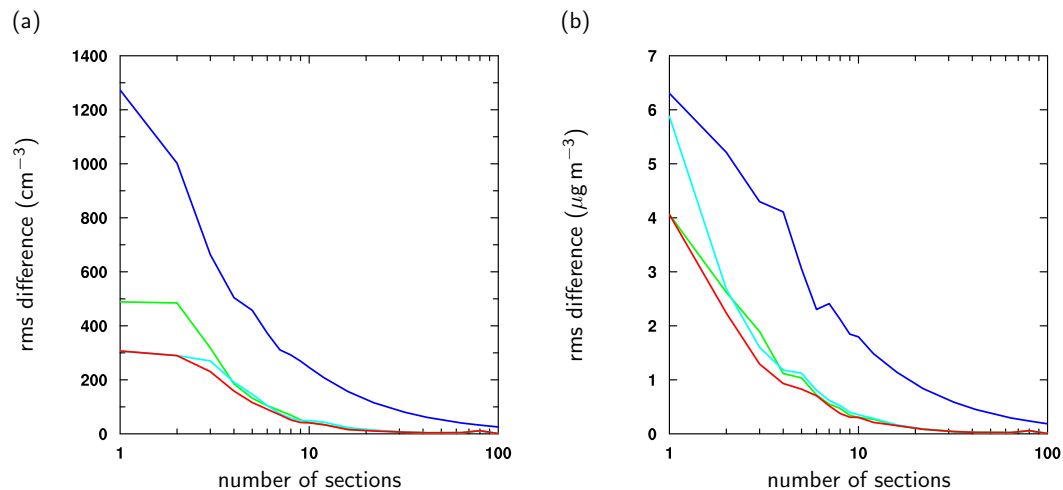


Fig. 4. Mean rms differences between the approximated and spline interpolated size distributions for aerosol number **(a)** and mass **(b)** for all samples from the NYC experiment. Blue lines refer to the bin approach and the other lines to the PLA method for optimal choice of $\psi_{m,i}$ (red), $\psi_{m,i}=1$ (cyan), and $\psi_{m,i}=4$ (green).

[Title Page](#)[Abstract](#)[Introduction](#)[Conclusions](#)[References](#)[Tables](#)[Figures](#)[◀](#)[▶](#)[◀](#)[▶](#)[Back](#)[Close](#)[Full Screen / Esc](#)[Print Version](#)[Interactive Discussion](#)

EGU

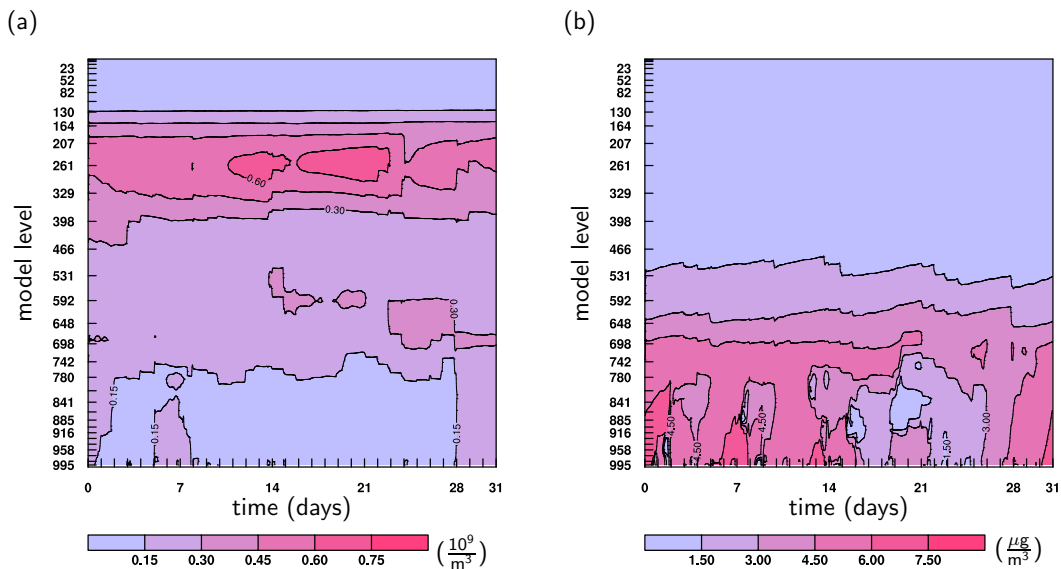


Fig. 5. Total aerosol number **(a)** and mass **(b)** concentrations in simulation for the ARM aerosol IOP, 1–31 May 2003. The model levels in the figure roughly correspond to pressure levels.

[Title Page](#)[Abstract](#)[Introduction](#)[Conclusions](#)[References](#)[Tables](#)[Figures](#)[◀](#)[▶](#)[◀](#)[▶](#)[Back](#)[Close](#)[Full Screen / Esc](#)[Print Version](#)[Interactive Discussion](#)

EGU

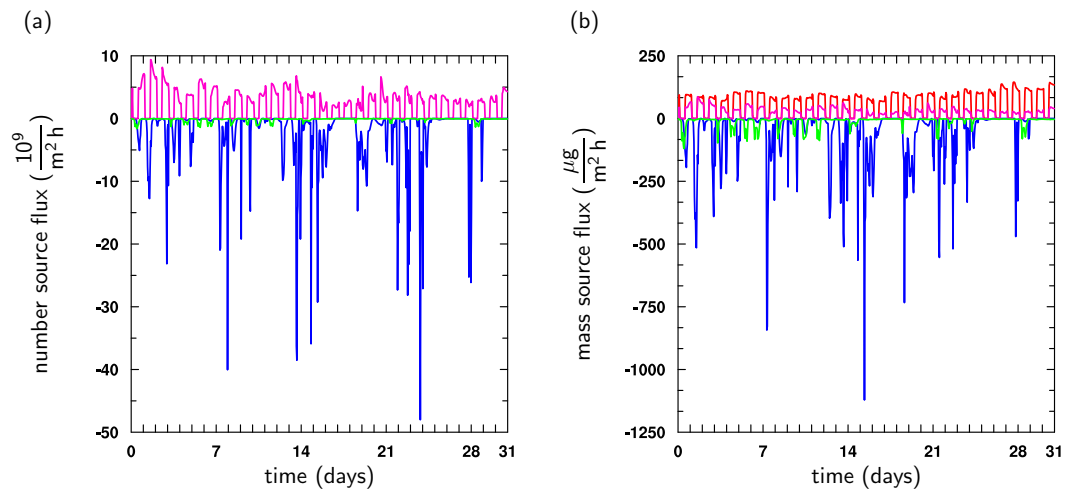


Fig. 6. Sources and sinks of column-integrated aerosol number **(a)** and mass **(b)** concentrations during the simulation. Sources are nucleation (pink lines), condensation (red line). Sinks are wet deposition (blue lines) and gravitational settling (green lines).

[Title Page](#)[Abstract](#)[Introduction](#)[Conclusions](#)[References](#)[Tables](#)[Figures](#)[◀](#)[▶](#)[◀](#)[▶](#)[Back](#)[Close](#)[Full Screen / Esc](#)[Print Version](#)[Interactive Discussion](#)

EGU

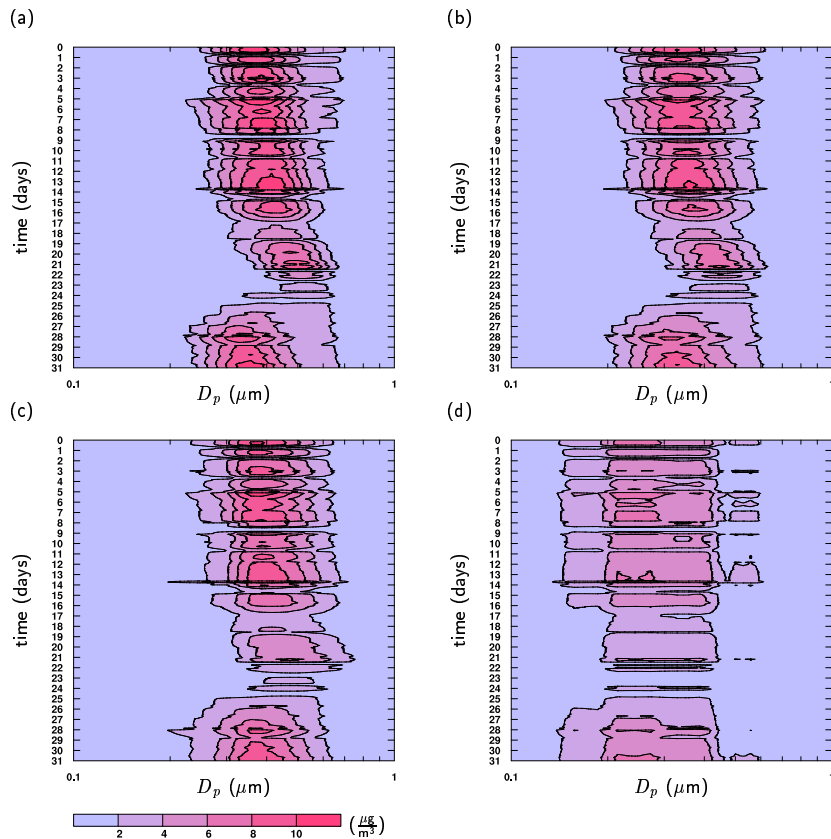


Fig. 7. Aerosol mass size distribution in the first model layer near the surface. The left column (a and c) is for results from simulations with the PLA method, the right column (b and d) is for results from simulations with the bin approach. Simulations with the PLA method are for 40 (a) and 3 sections (c) for an equal number of sections for aerosol number and mass. Simulations with the bin approach are for 80 (b) and 10 sections (d).

[Title Page](#)[Abstract](#)[Introduction](#)[Conclusions](#)[References](#)[Tables](#)[Figures](#)[◀](#)[▶](#)[◀](#)[▶](#)[Back](#)[Close](#)[Full Screen / Esc](#)[Print Version](#)[Interactive Discussion](#)

Piecewise log-normal approximation

K. von Salzen

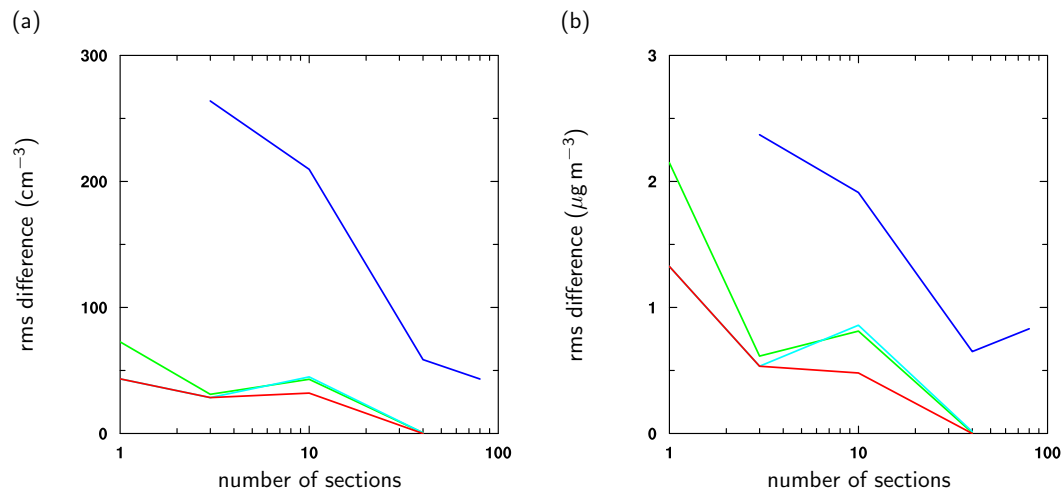


Fig. 8. Mean rms differences for simulated size distributions for aerosol number **(a)** and mass **(b)** in the first model layer. The differences are relative to the results of the simulation with the PLA method for 40 sections. Blue lines refer to the bin approach and the other lines to the PLA method for optimal choice of $\psi_{m,i}$ (red), $\psi_{m,i}=1$ (cyan), and $\psi_{m,i}=4$ (green).

[Title Page](#)[Abstract](#)[Introduction](#)[Conclusions](#)[References](#)[Tables](#)[Figures](#)[◀](#)[▶](#)[◀](#)[▶](#)[Back](#)[Close](#)[Full Screen / Esc](#)[Print Version](#)[Interactive Discussion](#)

EGU

Piecewise log-normal approximation

K. von Salzen

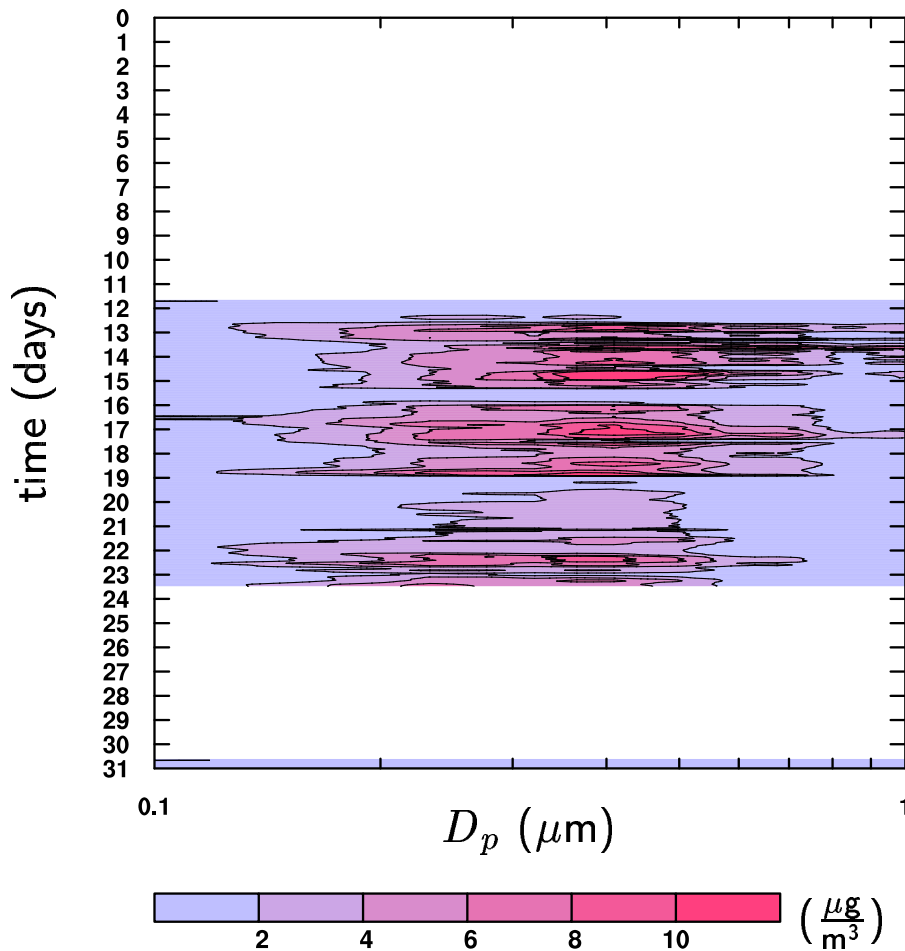


Fig. 9. Observed aerosol mass size distribution at the SGP site during the ARM aerosol IOP.

[Title Page](#)[Abstract](#)[Introduction](#)[Conclusions](#)[References](#)[Tables](#)[Figures](#)[◀](#)[▶](#)[◀](#)[▶](#)[Back](#)[Close](#)[Full Screen / Esc](#)[Print Version](#)[Interactive Discussion](#)

EGU